GPR Simulations of a Buried Concrete Wall for AlliedSignal

Zhubo Huang, Carl Leuschen, Christopher Allen and Richard Plumb

Radar Systems and Remote Sensing Laboratory
University of Kansas Center for Research, Inc.
2291 Irving Hill Road, Lawrence, Kansas 66045-2969, USA
913/864-4835 * Fax, 913/864-7789 * graham@rsl.ukans.edu

RSL Technical Report 11910-1

November 1996

Sponsored by:

AlliedSignal, Inc.
P. O. Box 419159, Kansas City MO 64141

PO 082G389580

GPR Simulations of a Buried Concrete Wall for AlliedSignal

Zhubo Huang, Carl Leuschen, Christopher Allen, Richard Plumb

November 1996

Sponsored by AlliedSignal, Kirtland Area Operations

GPR Simulations of a Buried Concrete Wall for AlliedSignal

1. Objective

The objective of this report is to present several computer simulations to determine if a hole in a buried concrete wall can be detected using a GPR. Numerical simulations were performed in both two- and three-dimensional spatial domains using the KU GPR simulator. We analyzed these simulations to find out (1) if a small hole could be detected by a GPR and (2) what kind of simulation (2-D or 3-D) is appropriate for such kind of application.

2. Specifications of the experiment

The geometry of the experiment to be simulated is shown in Fig. 1, according to the basic requirements by AlliedSignal.

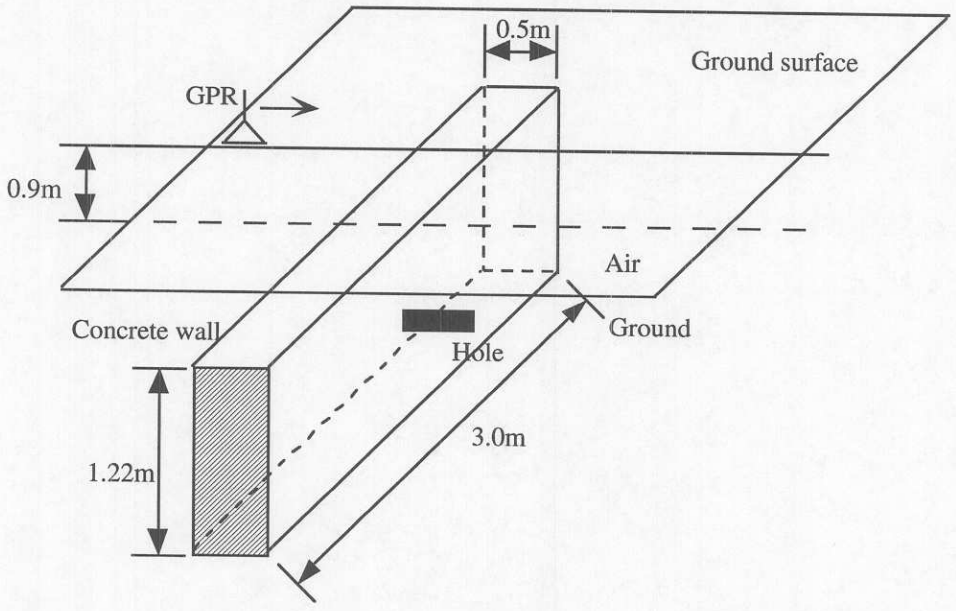

Figure 1: Experiment geometry.

The concrete wall is buried 0.90 m beneath ground. The dimensions of the wall are 0.5 m thick, 3.0 m long and 1.22 m wide. The GPR is working at a center frequency of 300 MHz with a bandwidth of 300 MHz. The GPR is moved along the ground surface across the center of the wall taking measurements at 0.1 m intervals on the ground surface. A hole is assumed to be 0.04 m x 0.04 m through the wall along its thickness, which is at 1.0 m below the top of the wall and offset 0.5 m from the center of the wall. The relative permittivity and conductivity of the concrete wall is 8.0 and 1.0×10^{-5} S/m, respectively. The relative permittivity and conductivity of the ground is 3.5 and 2.5×10^{-5} S/m, respectively.

3. Specifications of numerical simulations

The simulations were performed using the KU GPR simulator that was built using finite-difference time-domain method (FDTD) for electromagnetic scattering analyses. The simulations were performed in both two- and three-dimensional spatial domains. The two-dimensional simulations generally take much less simulation time and are good approximation for symmetric geometries.

Prior to the simulations, the FDTD cell size had to be determined for the KU GPR simulator. For the 300 MHz GPR used in the experiment, the simulator will use a time-domain pulse whose maximum significant frequency component is at 800 MHz. The corresponding wavelength in the ground is 0.2 m. In order to ensure the stability of FDTD, the cell size of the FDTD space is required to be 0.02 m, one tenth of the minimum wavelength that is specified by the wavelength of the maximum significant frequency.

A solution space for computer simulations was chosen to be 100 x 170 x 140 cells (2 x 2.5 x 3.5 m). The space was select to include the buried wall and sufficient surrounding space that is required to ensure accurate results. The wall contains 25 x 150 x 61 cells and is buried 45 cell beneath the ground. The GPR antenna is simply modeled by a current source, which adequately models a real antenna. Note that the KU GPR simulator can model more complex GPR antennas. The current source is a line source for two-dimensional space or a short dipole for three-dimensional space. The time-domain

behavior of the current source is specified by a time-domain pulse, a 4-ns double peak Gaussian pulse which yields the desired signal spectrum.

Characteristics of actual GSSI 300 MHz GPR antennas with baluns designed and fabricated by AlliedSignal personnel were measured and are presented in Appendix A. The results of these measurements relating to the simulation efforts were inconclusive.

4. Two-dimensional Simulations

The geometry of the two-dimensional simulation is shown in Fig. 2. The GPR antenna is modeled by a line source. The KU GPR simulator models the GPR as it takes measurement on the ground surface, moving perpendicular to the length of the concrete wall and crossing at the center of the wall. At each position along the ground, the line source launches a time-domain pulse and the returned electric fields are sampled at the point 2 cells away from the line source.

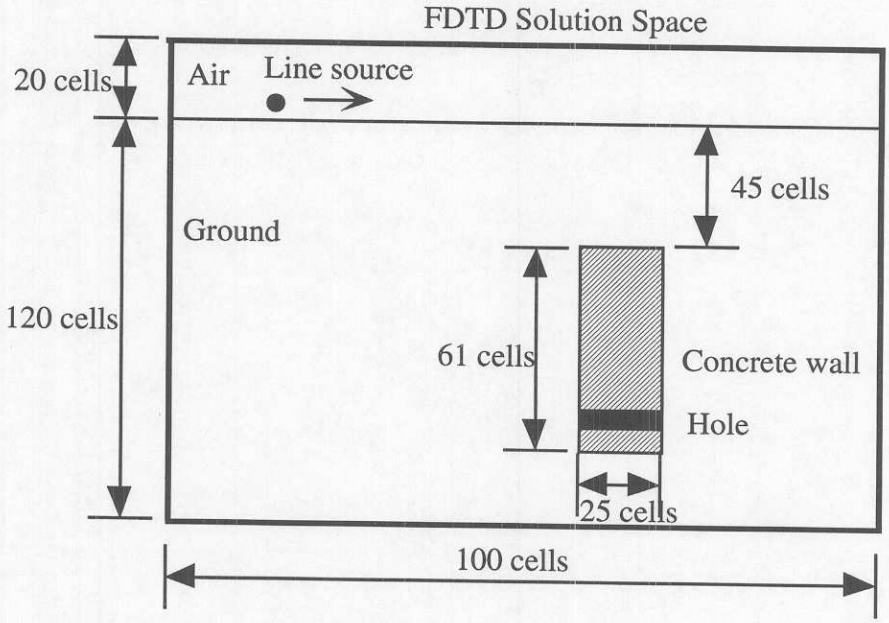

Figure 2: The geometry of two-dimensional simulation.

The simulation results for the wall without and with hole are shown in Fig. 3 and Fig. 4, respectively. These figures are displayed in wiggle format, where the horizontal axis corresponds to the position on the ground surface where the GPR takes measurements, the vertical axis is the range of radar return, and the size of wiggle represents the intensity

of radar return. This kind of wiggle plot shows radar returns of all single measurements in one plot, which is convenient to view the changes of radar returns as the GPR moving on the ground surface. Each curve in these figures represents a measurement at a field measurement point on the ground surface. In order to identify the responses due to the hole on the wall, Fig. 5 shows the difference between Fig. 3 and Fig. 4. Here, we can see that the response from the hole is significant.

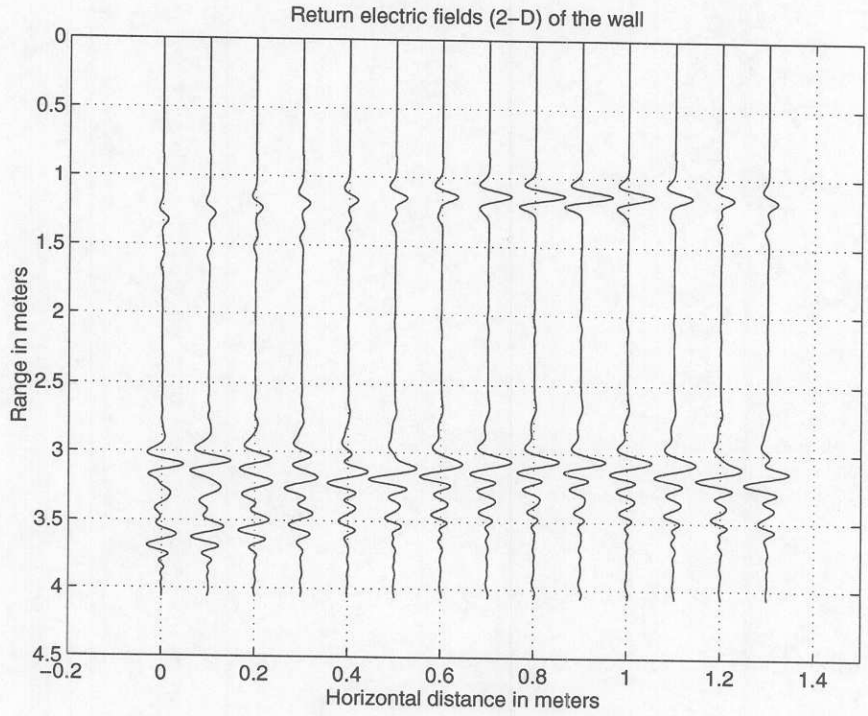

Figure 3: Two-dimensional simulation for the wall without a hole.

In Fig. 3, there are two strong responses from the concrete wall in each curve. The first one is mainly generated by the top face of the wall, and the second one is mainly due to the bottom face of the wall. In order to verify above conclusion, another simulation was performed. In this simulation, the GPR was located exactly above the wall and the vertical extent of wall was varied from 0.1 m to 1.8 m with fixed location of the top face of the wall. The simulation result is shown in Fig. 6. Here, we see that the first response remains same, however, the second response has different time delays while the vertical extent of the wall varies. This would imply that the wall (having a higher permittivity than the background material) is acting as a waveguide, effectively guiding the waves and

the reflection from the bottom surface of the wall changes with the vertical extent of the wall.

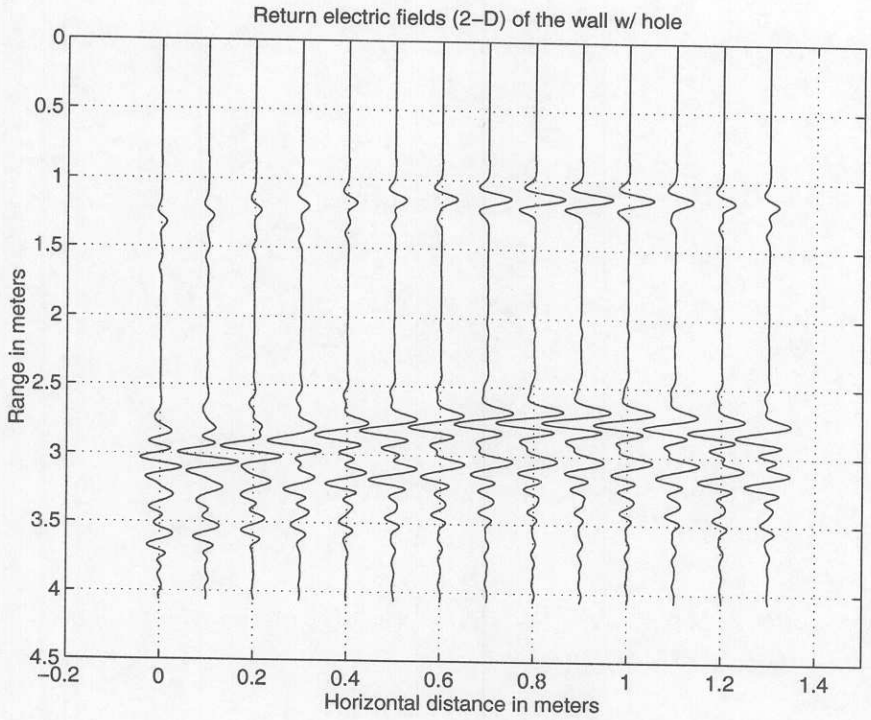

Figure 4: Two-dimensional simulation for the wall with a hole.

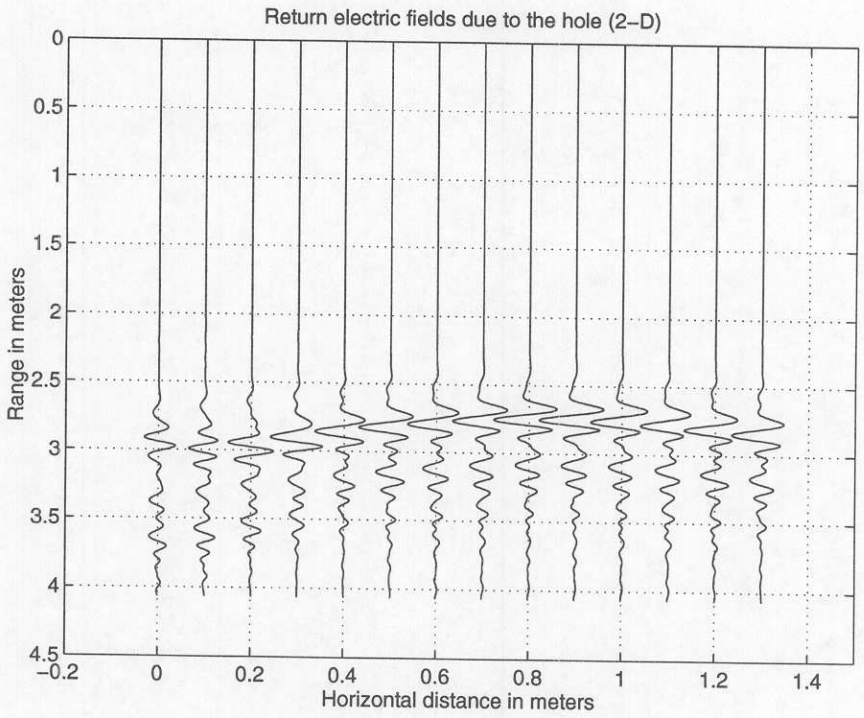

Figure 5: The response due to the hole on the wall, 2-D situation.

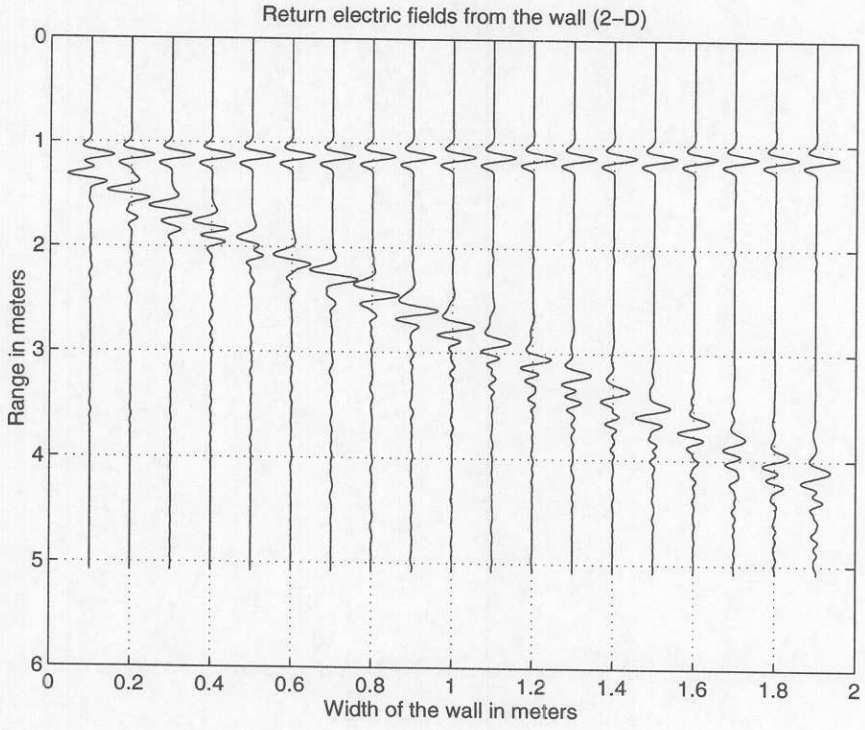

Figure 6: Simulated GPR responses from a variety of walls having different vertical extents.

5. Three-dimensional Simulations

To perform three-dimensional simulations, a dipole is used to model the GPR antenna. The simulation geometry is shown in Fig. 7. The dipole is moved on the ground surface across the buried wall. In this case, a time-domain pulse is launched from the dipole and return electric fields are sampled at the point two cells away from the dipole.

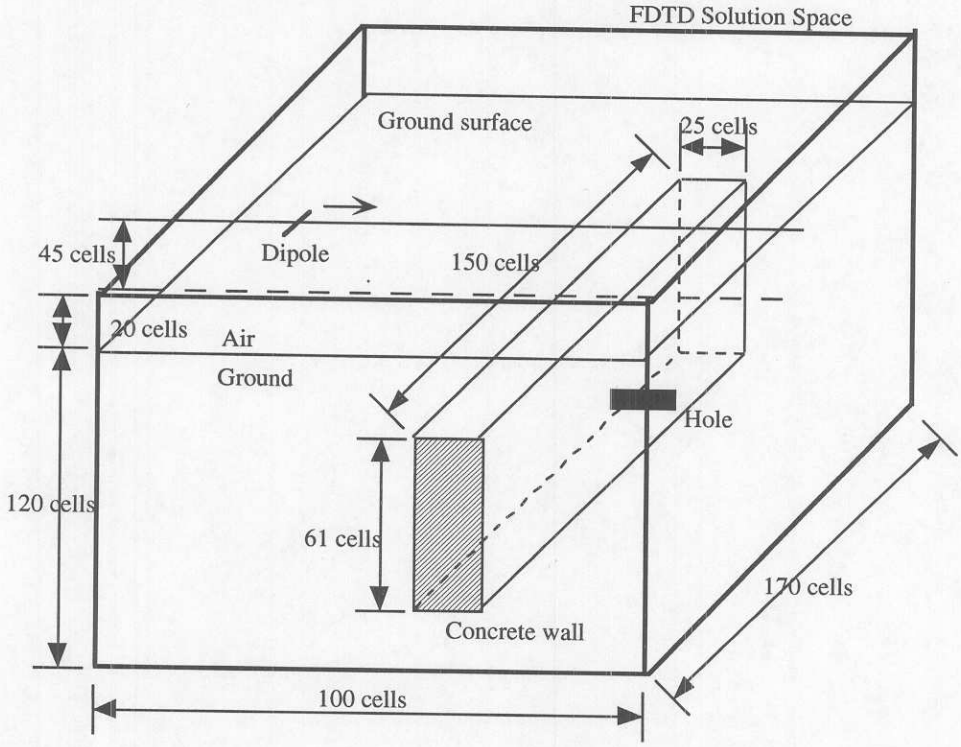

Figure 7: The geometry of three dimensional simulation.

The simulation results for the wall without and with a hole are shown in Fig. 8 and Fig. 9, respectively. Fig. 10 shows the difference between Fig. 8 and Fig. 9, however the difference has been amplified by a factor of 15, which indicates that the responses from a small hole is weak.

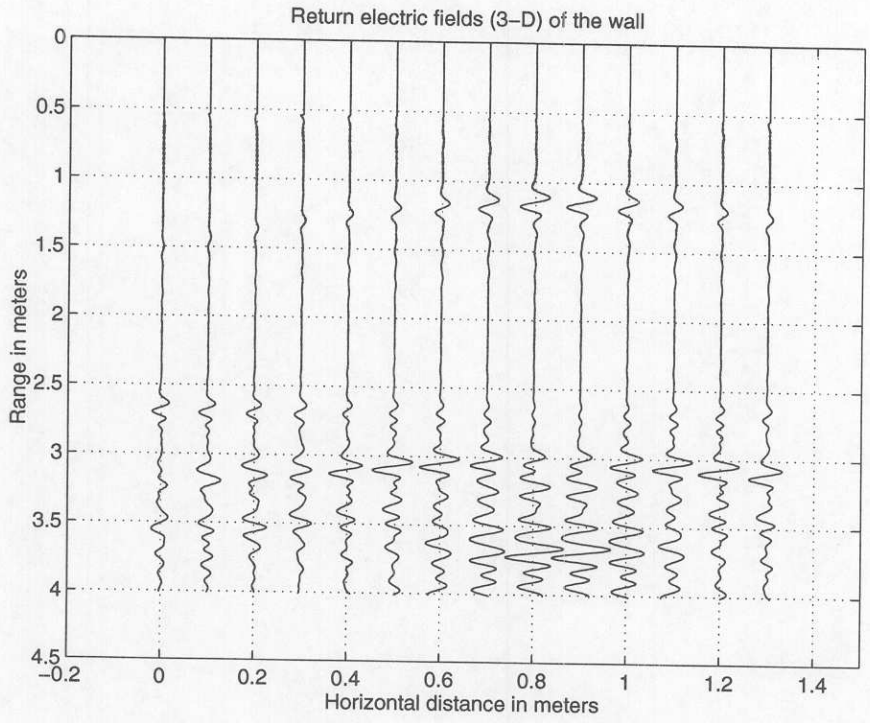

Figure 8: Three-dimensional simulation for the wall without a hole.

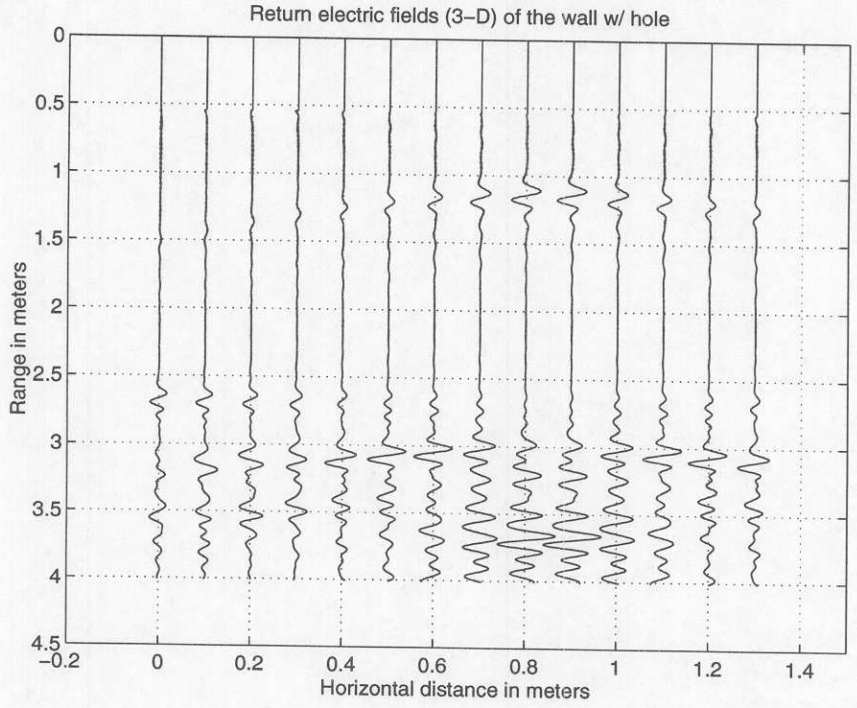

Figure 9: Three-dimensional simulation for the wall with a hole.

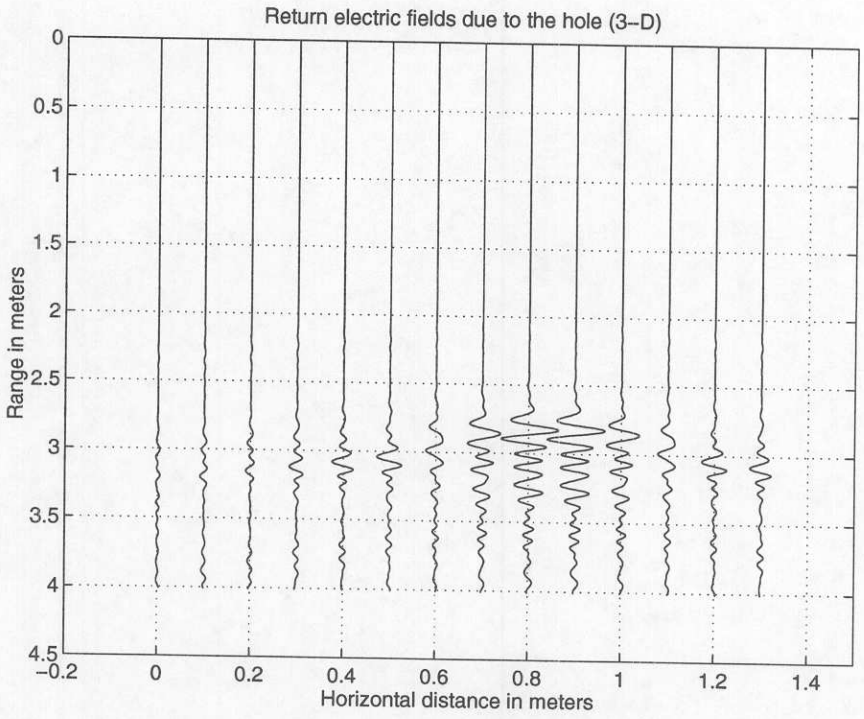

Figure 10: The response due the hole on the wall, 3-D situation.

6. Discussion

Both two- and three-dimensional simulations give similar results in the main part of radar return responses, which appear at about one meter in range. For the multiple reflections between the ground surface and the wall, which appear at about three meters in range, the two simulations give quite different results, which is mainly due to different dimensions of simulation space.

These simulations show that a small hole can be detected by a GPR. Two-dimensional simulation shows stronger responses from the hole, because a hole in the two-dimensional space presents a gap in the whole wall thickness. Three-dimensional simulation is closer to the actual situation than two-dimensional simulation. However, the three-dimensional simulation shows the scattered fields from the hole on the wall are very weak. Therefore, additional post-processing of radar signal is needed in actual experiments.

The simulation time for these two simulations are very different. In order to obtain one curve in these wiggle plots, a complete FDTD run is required. A FDTD run for the

two-dimensional simulation takes about 3-minutes of CPU time on a Pentium-90 PC. However, a FDTD run for the three-dimensional simulation requires about 7-hours of CPU time. Therefore, the two- and three-dimensional simulations shown in this document requires 42 minutes and 98 hours of CPU time, respectively. On the other hand, during 98 hours of the whole three-dimensional simulation, we found out the Pentium-90 PC machine had an instability problem for a long-time simulation (crashed during the simulation). Therefore, the actual three-dimensional simulation was performed on a Digital workstation, DEC3000/400.

In conclusion, a small hole can be detected by a GPR, two-dimensional simulation can provide fundamental information about real experiment, and three-dimensional simulation generates more accurate results with the cost of more computation time and computer memory. As a suggestion, a real antenna modeling is required to get more accurate results.

7. Processing the Raw Data

In order create an image of the wall, a signal processing technique was applied to the two-dimensional simulated data to focus the collected measurements back to their source. The method involved using a reverse-time algorithm similar to that of f-k migration (see Appendix B for more details). The method used is based on an assumption commonly known as the exploding reflector model in which the returned signals are assumed to have originated from subsurface scatterers and propagated to the receiving antenna. An image is them constructed by re-propagating the waves from the surface back into the ground which was assumed to have a relative permittivity of 3.5 and a conductivity of 2.5×10^{-5} S/m. The waves will then add constructively where a target exists and destructively elsewhere. Fig. 11 below shows the raw data and the image resulting from applying this technique.

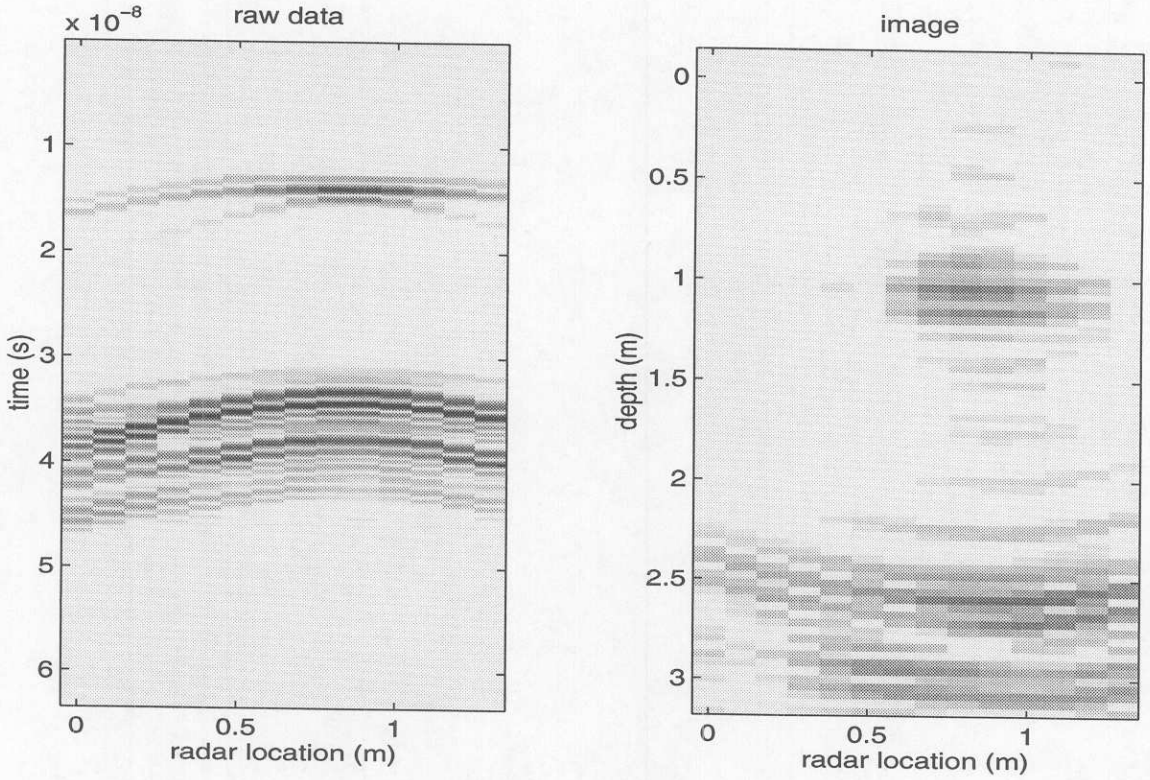

Figure 11: Raw 2-D simulated GPR data and the focused image resulting from the application of this technique.

As shown in the figure, the algorithm was able to focus the first hyperbola but not the second. Since this algorithm only takes into account the background permittivity of the ground and not the scatter when re-propagating the waves back into the ground, the inability to focus the second hyperbola was expected. This result indicates that the second hyperbola seen in the raw data is an effect of the wall acting as a waveguide.

In conclusion, the imaging technique was able to determine the location and give a rough estimate of the lateral size of the wall. The relative permittivity and shape were not apparent in the image which was expected due to the nature of the algorithm.

Appendix A

Antenna and Balun Measurements

To evaluate the effectiveness of the antennas and the baluns the voltage standing wave ratio (VSWR) and transmission characteristics were measured over their useful frequencies. The VSWR of each antenna-balun combination was measured using a HP network analyzer with the antenna placed on the surface of a sand-air interface. The network analyzer was calibrated at the point where the cable attached to the balun. The VSWR for each balun configuration is shown on the following two pages. The third plot shows the transmission characteristic of the two antennas when placed opposite each other. The configurations for both the VSWR and transmission measurements are shown below.

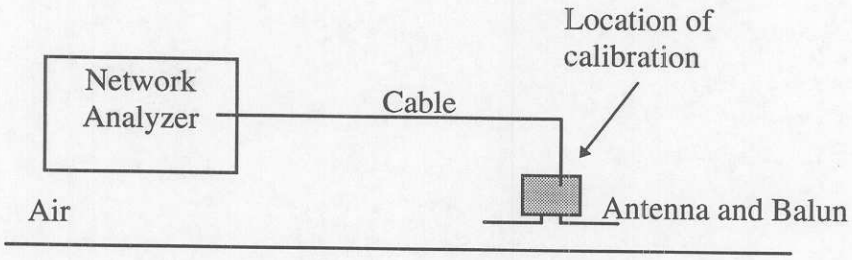

VSWR Measurement Configuration

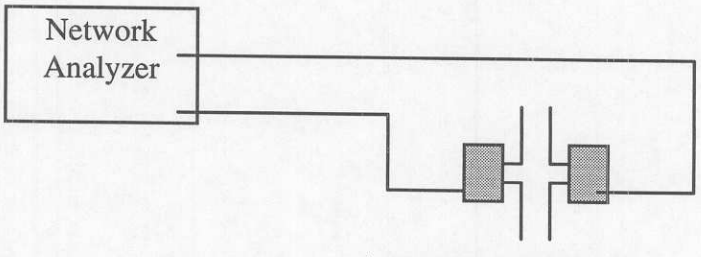

Transmission Measurement Configuration

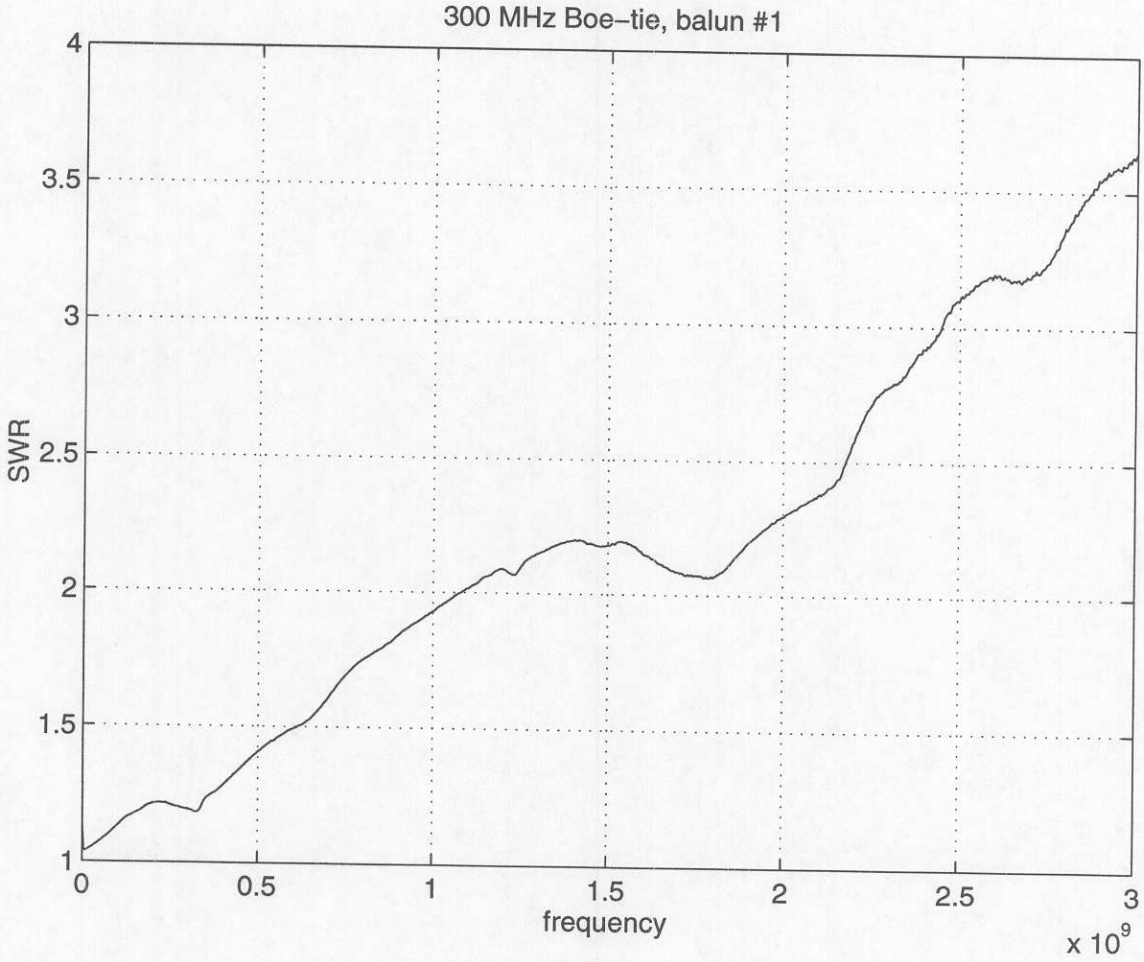
300 MHz Boe–tie, balun #1
SWR
frequency
x 10^9
4
3.5
3
2.5
2
1.5
1
0
0.5
1
1.5
2
2.5
3

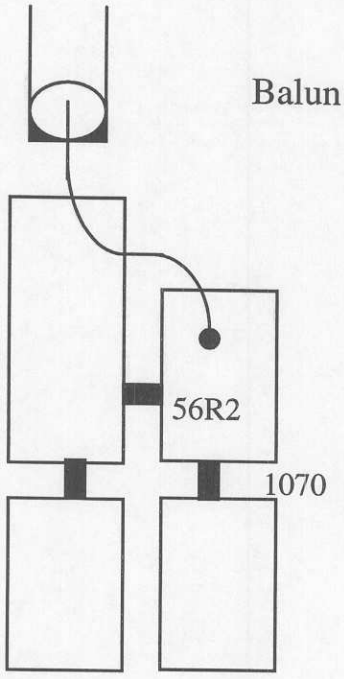
Balun #1
56R2
1070

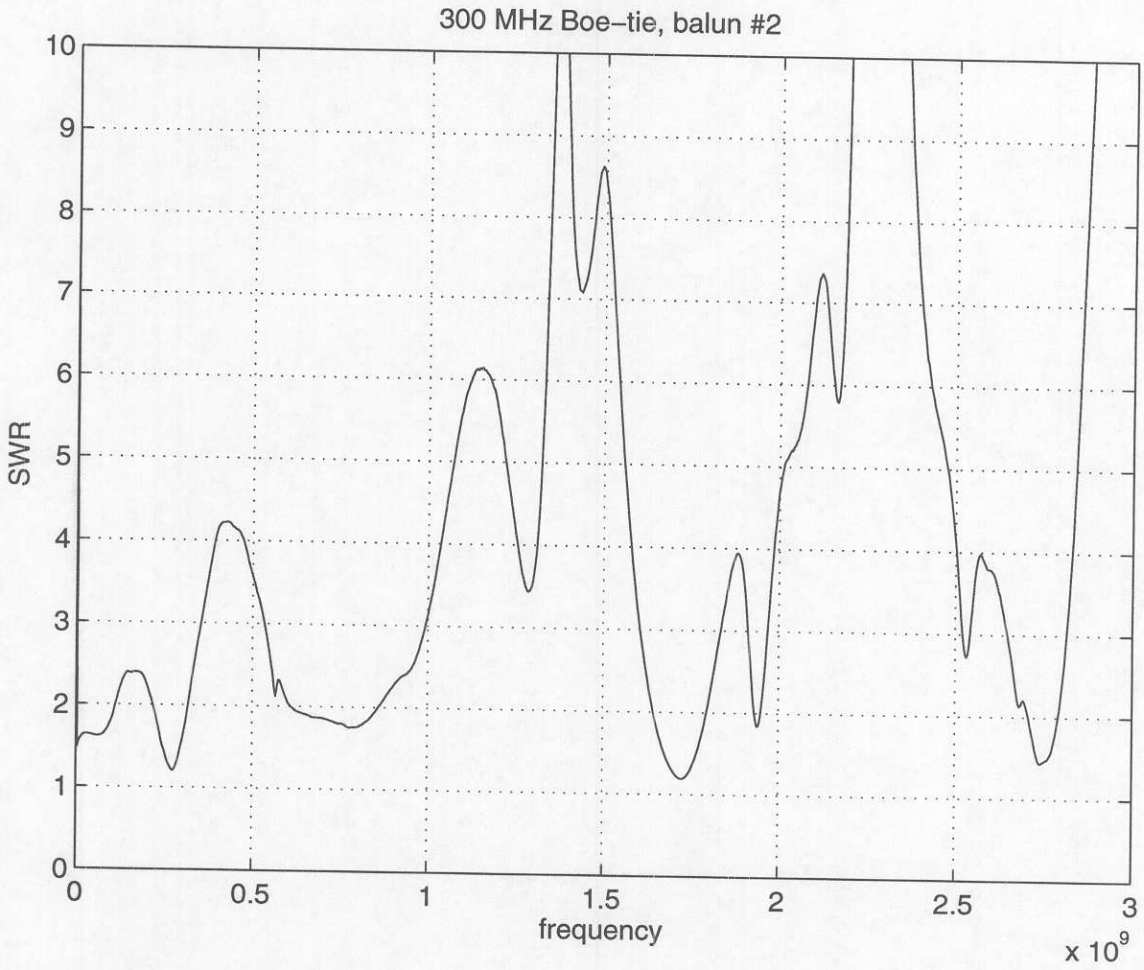
300 MHz Boe–tie, balun #2
SWR
frequency
x 10^9
0
1
2
3
4
5
6
7
8
9
10
0
0.5
1
1.5
2
2.5
3

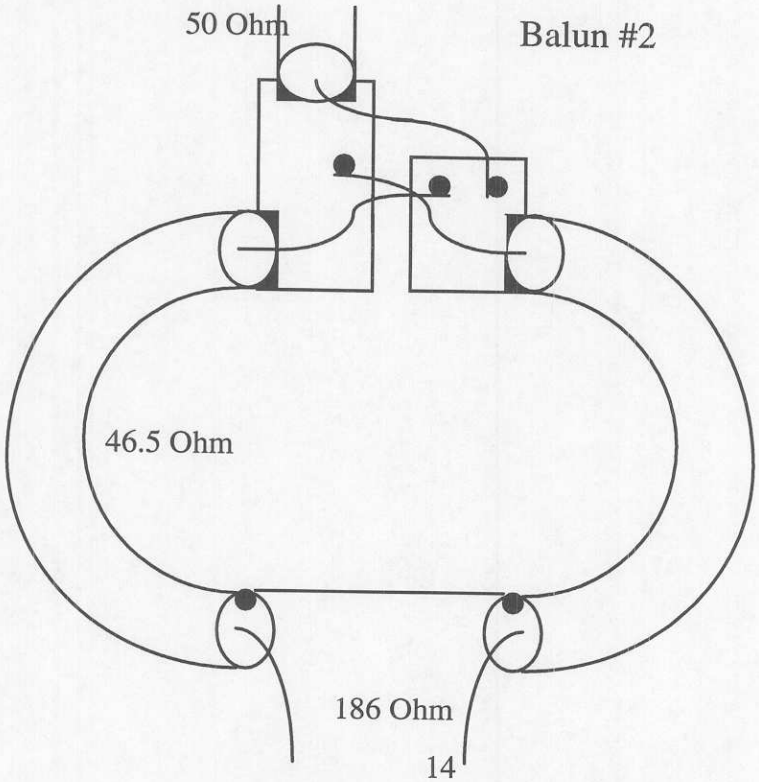
50 Ohm
Balun #2
46.5 Ohm
186 Ohm

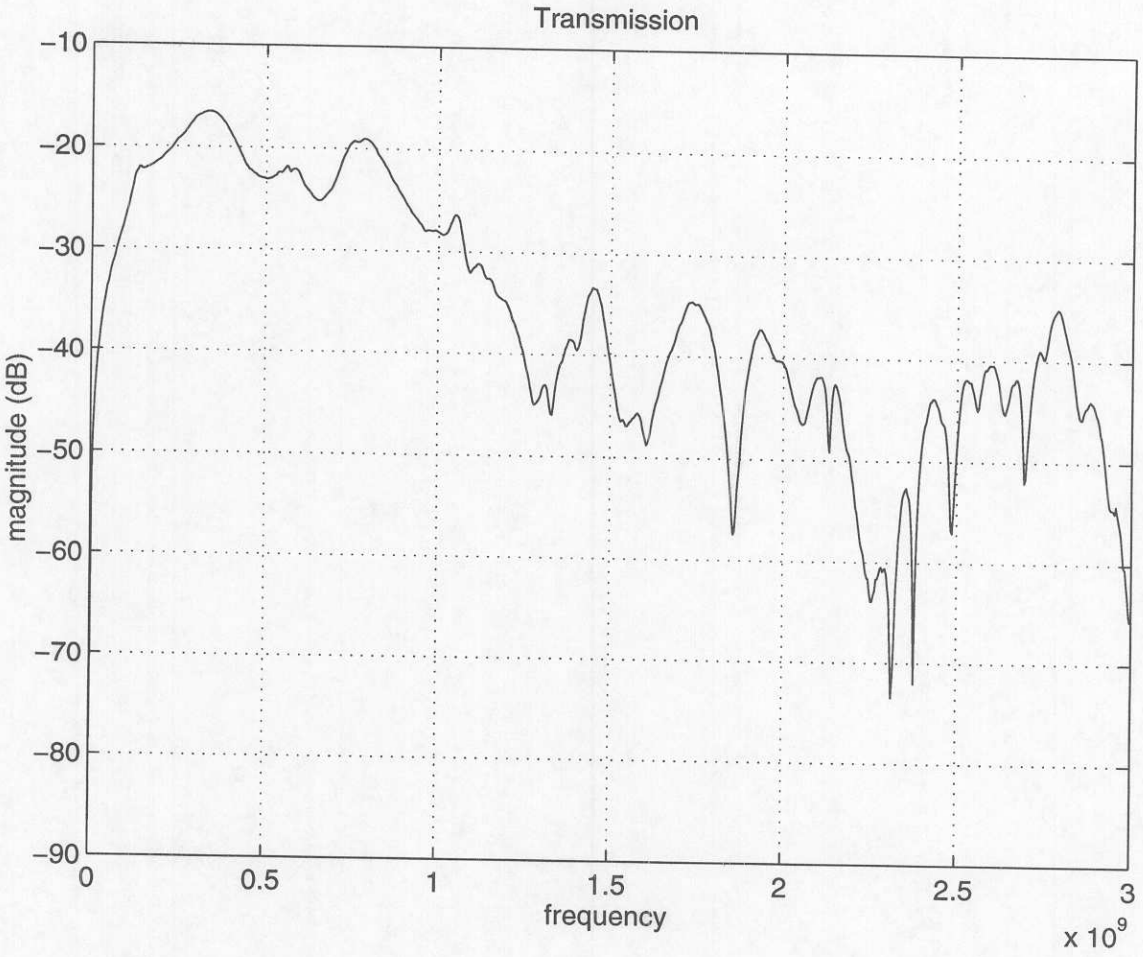
Transmission
−10
−20
−30
−40
−50
−60
−70
−80
−90
magnitude (dB)
0
0.5
1
1.5
2
2.5
3
frequency
x 10^9

Appendix B

Exploding (Radiating) Reflector Model

Assumptions made prior to data processing in order to image the reflected signals as being signals generated by sources located in the subsurface.

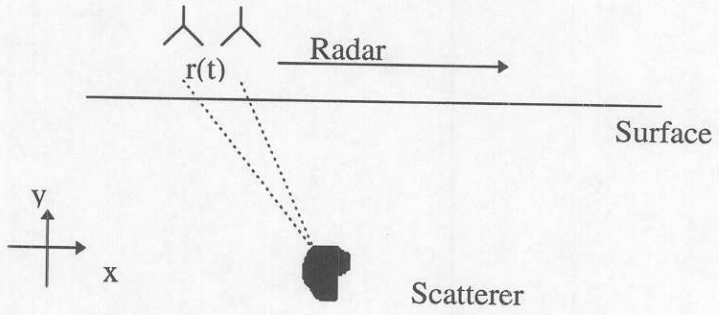

- by using a very small antenna separation, the reflected signal, r(t), can be seen as being generated by the scatterer and propagating at one half the speed to the receiving antenna.

- by reversing the received signal in time, r(t) = r(-t), the signal is introduced at the radar location and propagated back to the source at one half the propagation speed.

- an image is created by evaluating the field at t = 0.

B.1 Development

Since the received signal, r(t), is propagated back into the space as r(-t), an equivalent current density, J(x,-t) which is equal to r(-t) at the radar location x, is introduced in the presence of no known scatterers.

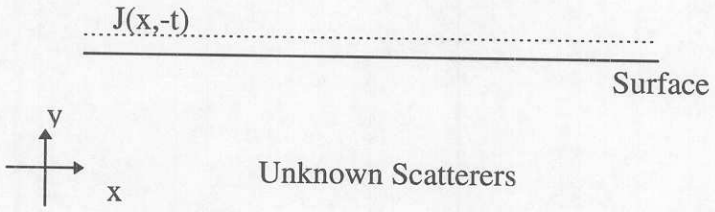

Now to obtain an image, two things must be done.

1. The current density J(x,-t) must be introduced into the space and evaluated at locations in the subsurface.
2. The wave must be propagated at one half the speed and evaluated at a time t = 0.

B.2 Introducing J(x,-t) into a Two-dimensional Space

J(x,-t) is introduced into the space by first converting to the frequency domain through a fourier transform and then by evaluating the differential equation shown in (2).

$$J(x,f) = F\{J(x,-t)\} \tag{1}$$

$$\left\{\nabla^2 + k(y)^2\right\} g_1(x,y) = -\delta(y) J(x,f) \tag{2}$$

Notice in equation (2) that k is restricted to being a function of y, allowing the introduction of a layered earth.

With prior knowledge of the solution to (3), the function $g_1(x,y)$ can be obtained by a convolution of $g_0(x,y)$ and J(x,f) or by multiplication in the spatial frequency, kx, domain shown in (4) through (6).

$$\left\{\nabla^2 + k(y)^2\right\} g_0(x,y) = -\delta(y)\,\delta(x) \tag{3}$$

$$\left\{\frac{d^2}{dx^2} + k(y)^2 - kx^2\right\} g_0(kx,y) = -\delta(y) \tag{4}$$

$$J(x,f)\left\{\frac{d^2}{dx^2} + k(y)^2 - kx^2\right\} g_0(kx,y) = -\delta(y) J(x,f) \tag{5}$$

$$g_1(kx,y) = J(x,f)\, g_0(kx,y) \tag{6}$$

If the polarization of the antennas are in the z direction and thus the vector J(x,f) is also in the z direction, the electric field is obtained as being directly proportional to the function $g_1(x,y)$.

$$E(x,y) = -j\omega\mu g_1(x,y) \tag{7}$$

B.3 Wave Propagation at One-Half Speed and Evaluation at t=0

Since the fields are evaluated in the frequency domain, finding the field at a time equal to zero is accomplished simply by taking an average of all the frequency components without a phase shift or evaluating the inverse Fourier transform at t=0.

By introducing J(x,-t) at twice the rate or using J(x,-2t) and keeping the propagation speed the same, a similar effect of reducing the propagation speed is accomplished. This is done in the inverse Fourier transform by increasing the frequency by a factor of two.

$$r(t) = \int R(f)\exp\{j2\pi ft\}dt \tag{8}$$

$$r(2t) = \int R(f)\exp\{j4\pi ft\}dt \tag{9}$$

B.4 Simulation

To verify this technique was implemented using fdtd simulated data of a buried pipe. Figures:

1. The basic geometry.
2. The scattered field.
3. The current density at 600 MHz to be applied to $g_0(x,y)$ at 2*f=1.2 GHz.
4. The resulting image at 1.2 GHz.
5. The final image (intensity).
6. The final image (surface).

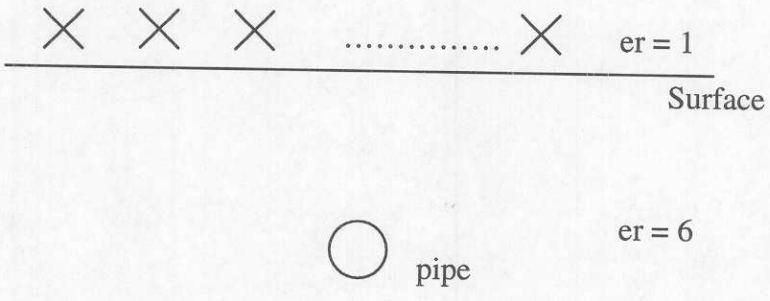

Fig. B-1.

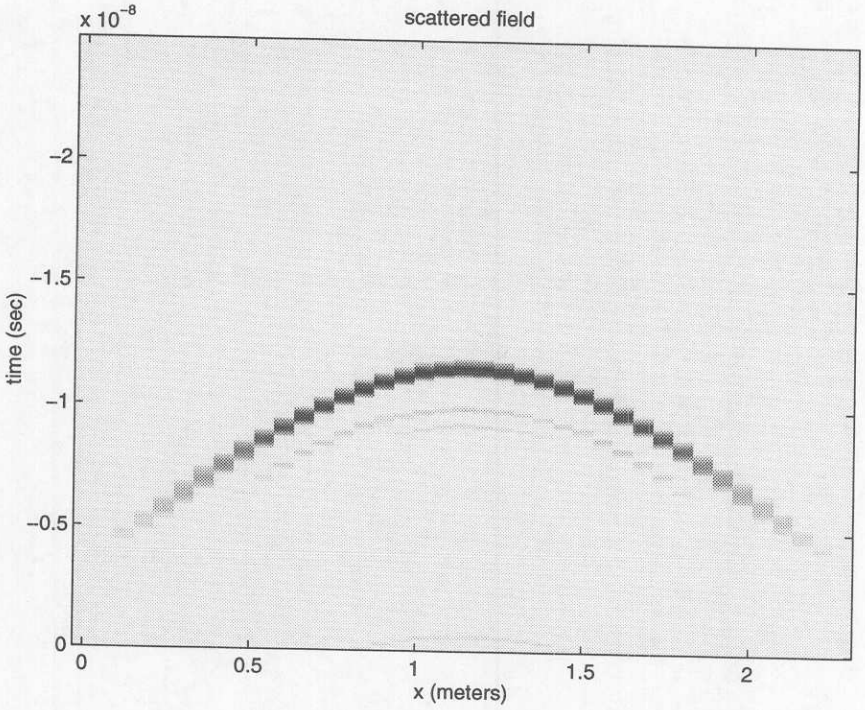
x 10^-8
scattered field
time (sec)
x (meters)

Fig. B-2.

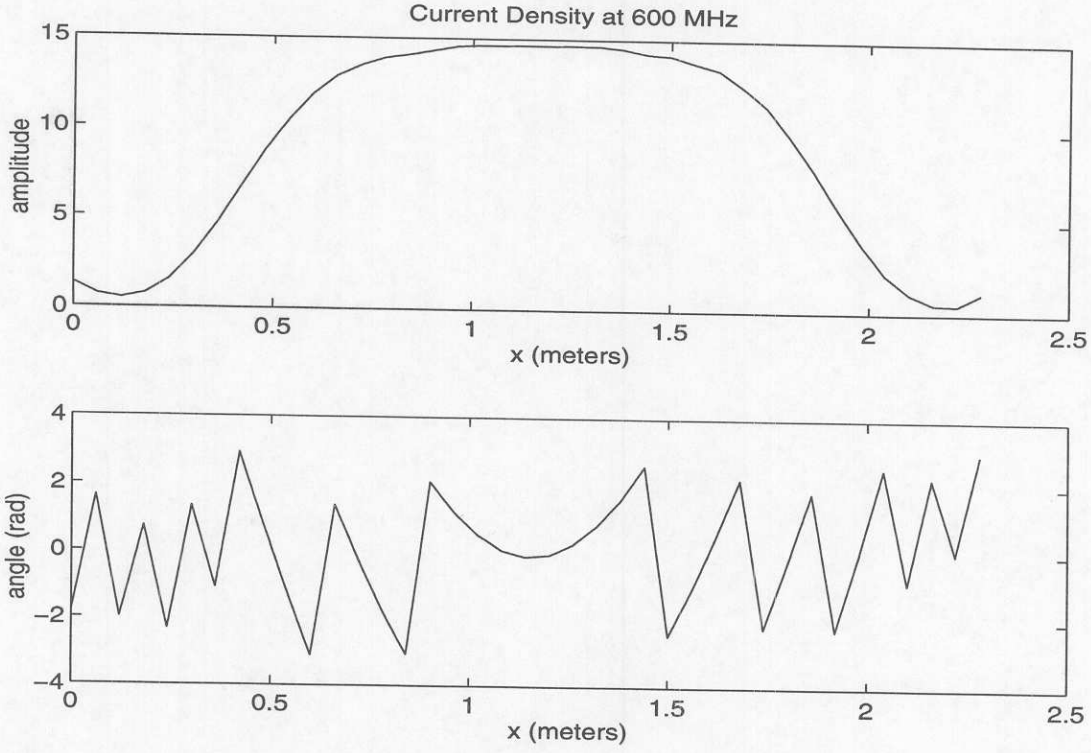
Current Density at 600 MHz
amplitude
x (meters)
angle (rad)
x (meters)

Fig. B-3.

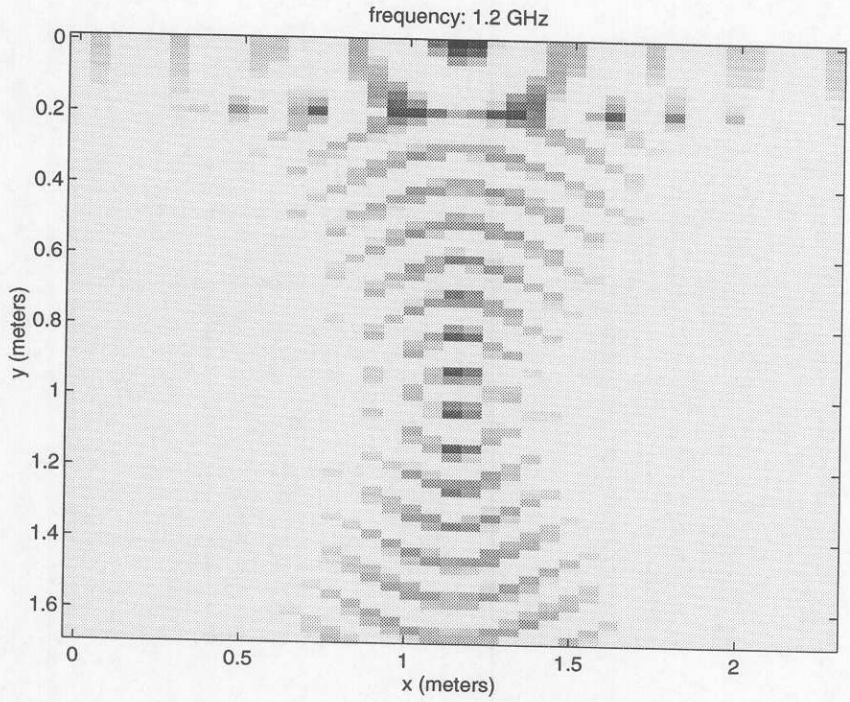
frequency: 1.2 GHz
0
0.2
0.4
0.6
0.8
1
1.2
1.4
1.6
y (meters)
0
0.5
1
1.5
2
x (meters)

Fig. B-4.

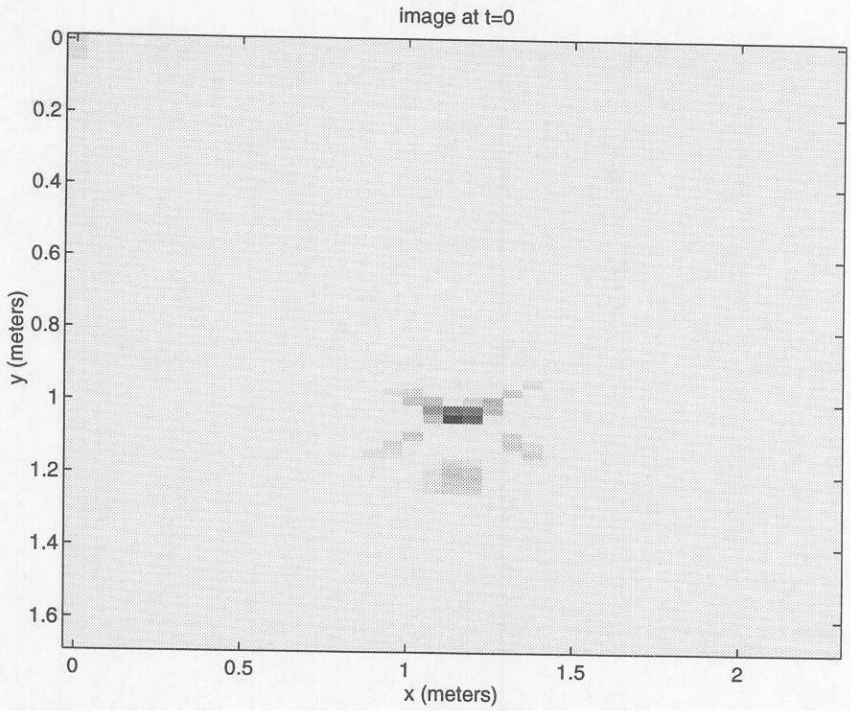
image at t=0
0
0.2
0.4
0.6
0.8
1
1.2
1.4
1.6
y (meters)
0
0.5
1
1.5
2
x (meters)

Fig. B-5.

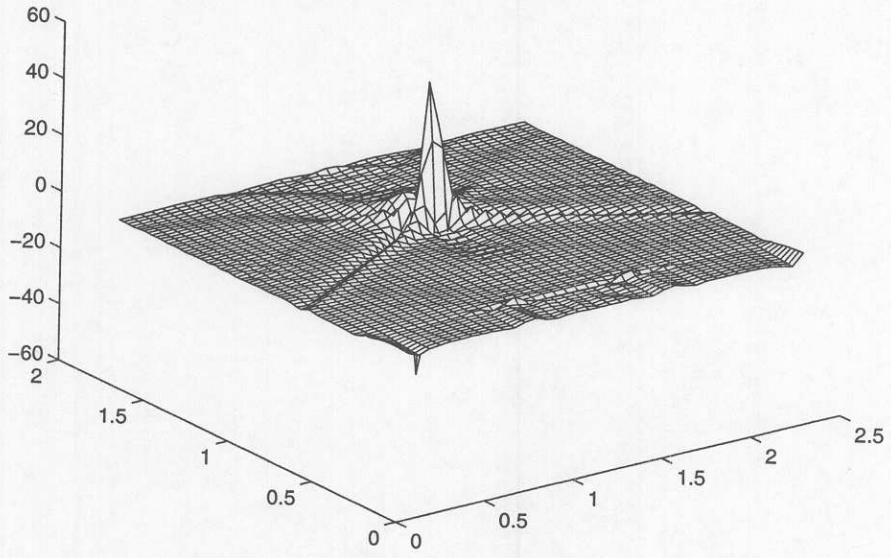

Fig. B-6.